ELSEVIER

Materials Science and Engineering B79 (2001) 247–250

MATERIALS SCIENCE & ENGINEERING B

www.elsevier.com/locate/mseb

Letter

Morphology and electrochemical properties of $LiMn_2O_4$ powders derived from the sol–gel route

Chung-Hsin Lu *, Susanta Kumar Saha

Department of Chemical Engineering, National Taiwan University, Taipei, 106 Taiwan, ROC

Received 4 September 2000

Abstract

Spinel-lithium manganese oxide ($LiMn_2O_4$) powders are prepared by the sol–gel method using polyvinyl alcohol (PVA) in this study, and evaluated as a positive electrode material for Li-ion batteries. PVA helps to maintain the homogeneity of the system in the precursors and thereby facilitates the formation of monophasic powders. The average primary particle size of the calcined $LiMn_2O_4$ powders decreases with an increase in the amount of PVA used in solution. Increasing the amount of PVA also results in a rise in the discharge capacity at 25°C because of the large interface area of small particles. On the other hand, the discharge capacity of the small $LiMn_2O_4$ particles suffers markedly capacity fading when the batteries are operated at elevated temperatures.

Keywords: Homogeneity; Sol–gel method; Polyvinyl alcohol; Li Mn_2O_4

1. Introduction

Nowadays, the demand for rechargeable batteries with high energy density and high voltage has increased rapidly due to the advancement and popularity of portable electronic devices. Lithium manganese oxide ($LiMn_2O_4$) is a promising cathode material for lithium ion batteries because of its low cost and lower toxicity compared with the layered oxides $LiCoO_2$ and $LiNiO_2$. For the consideration of practical application, it is important to produce $LiMn_2O_4$ powders with excellent capacity and cyclability. The electrochemical properties of $LiMn_2O_4$ powders strongly depend on its synthesis process. The $LiMn_2O_4$ powders are usually prepared by the solid-state reaction [1–8]. This process requires extensive mechanical mixing, extended grinding, and prolonged heating time. These synthesis conditions inevitably result in the unexpected grain growth of the spinel particles. To achieve good efficiency of Li utilization at high current rates and improve the reliability of lithium secondary batteries, several chemical methods have been introduced to synthesize cathode materials with good homogeneity, uniform morphology and a narrow size distribution. The chemical methods such as co-precipitation [9], emulsion drying [10,11], sol–gel [12] and the Pechini process [13] have been developed to obtain the homogeneous $LiMn_2O_4$ powders with small average particle size.

For simplifying the synthesis process, we have developed a new sol–gel method for preparing the spinel $LiMn_2O_4$ powder with high capacity and good cycling behavior. In this process, appropriate ratios of cations are dissolved in water, and then the aqueous solution is mixed with polyvinyl alcohol (PVA) solution. The solution is evaporated from gel and subsequently dried to become precursor powder. The purpose of the study is to prepare homogeneous and monophasic $LiMn_2O_4$ powder. The charge–discharge characteristics of the cathode are also evaluated to examine the effects of particle size on the capacity and stability of $LiMn_2O_4$ powders.

---

* Corresponding author. Fax: + 886-2-3623040.

0921-5107/01/$ - see front matter © 2001 Elsevier Science B.V. All rights reserved.
PII: S0921-5107(00)00530-4

2. Experimental

A solution containing a stoichiometric mixture of reagent grade lithium nitrate and manganese nitrate hexahydrate was firstly prepared. The concentration of the solution was maintained at 1 M with respect to metal ions. An aqueous solution of PVA was prepared by dissolving it in deionized water. The PVA solution was then added into the mixed metal nitrate solution with thorough stirring. The molar ratio of the metal ions to vinyl alcohol monomer units of PVA in the starting solution was maintained at 1:2 (sample A) and 2:1 (sample B), respectively. The resulting viscous solution of metal nitrate and PVA mixture was evaporated with continuous stirring. The evaporated mass was then heated at various temperatures ranging from 400°C to 800°C.

TG/DTA studies of the evaporated powders were performed at a heating rate of 10°C min^{-1} in air. The FTIR spectra of the evaporated and heated powders were recorded from 400 to 2000 cm^{-1}. An X-ray diffractometer with Ni-filtered CuK_α radiation was used for the identification of the crystalline phases of the heat-treated powders. Transmission electron microscopic studies of the heat-treated powders were carried out using an electron microscope. The electrochemical behavior of the obtained $\mathrm{LiMn_2O_4}$ powders was examined in a test cell. Lithium foil was used as the anode. 1 M $\mathrm{LiPF_6}$ in ethylene carbonate/dimethyl carbonate (volume ratio = 1:1) was used as the electrolyte solution. Cells were charged and discharged at 0.2 mA cm^{-2} within the potential range of 3.0 and 4.3 V.

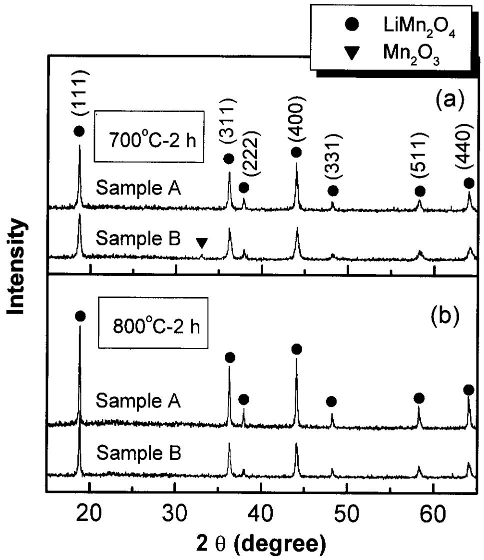

Fig. 1. XRD patterns for the (a) 700°C- and (b) 800°C-calcined powders obtained from precursor solutions having the molar ratio of the metal ions to the monomer units of PVA equal to 1:2 (sample A) and 2:1 (sample B).

3. Results and discussion

Results of TG/DTA analysis indicate the formation of lithium manganese oxide at 400°C, at which temperature the precursor has attained a stable weight on TGA curve. This observation is also supported by the FTIR results. Only two characteristic vibrational bands at 495 and 610 cm^{-1}, which correspond to metal oxygen bonds, are observed in the spectra of the powder heat-treated at 400°C or higher temperature. Fig. 1 shows the XRD patterns of $\mathrm{LiMn_2O_4}$ powders of samples A and B calcined at 700°C and 800°C in air. It is confirmed by the XRD patterns that only spinel $\mathrm{LiMn_2O_4}$ crystalline phase is formed in sample A at both temperatures. All diffraction peaks for these calcined powders are assigned to the diffraction indices of $\mathrm{LiMn_2O_4}$ spinel phase. However, the 700°C calcined powder of sample B exhibits both spinel $\mathrm{LiMn_2O_4}$ phase and a trace of $\mathrm{Mn_2O_3}$ phase. This impurity phase completely disappears after calcining the sample at 800°C. Precursor powder of sample B is assumed to be less homogeneous which may be the reason for the appearance of $\mathrm{Mn_2O_3}$ impurity phase at low temperatures. Sufficient amount of PVA is required for the formation of polymer matrix with a whole range of homogeneously trapped metal ions in gel [14,15]. When the amount of PVA is insufficient, the homogeneity of the cation ions in the gel is poor (such as in sample B); therefore, certain regions lack of lithium ions will produce $\mathrm{Mn_2O_3}$ phase. Furthermore, homogeneous distribution of the metal ions in the precursor powder reduces the diffusion distance among cation ions during heat treatment. This also accelerates the formation of monophasic spinel $\mathrm{LiMn_2O_4}$

Fig. 2 shows the transmission electron micrographs of 800°C-calcined powders of samples A and B. Calcined powders of both systems are loosely bound agglomerates of nanosized particles with a spherical morphology. 800°C-calcined powder of sample A is comparatively smaller than that of sample B. The average primary particle sizes of calcined samples A and B are 50 and 120 nm, respectively. The above observations reveal that the powder prepared by this method has much smaller particle size and narrower particle size distribution than that obtained by solid state [8] and other solution method [10]. During the heating of the precursor powder, CO, $\mathrm{CO_2}$, and $\mathrm{H_2O}$ are generated by the decomposition of organic species, which facilitate the formation of the dispersed and nanosized particles [16,17]. With a decrease in the amount of PVA used in sample B, the amount of generated gases is decreased, thereby resulting in an increase in the particle size.

Fig. 3 shows the charge–discharge curves of 800°C-calcined powders of sample A as the cathode material operated at 25°C and 55°C. All the samples exhibit two

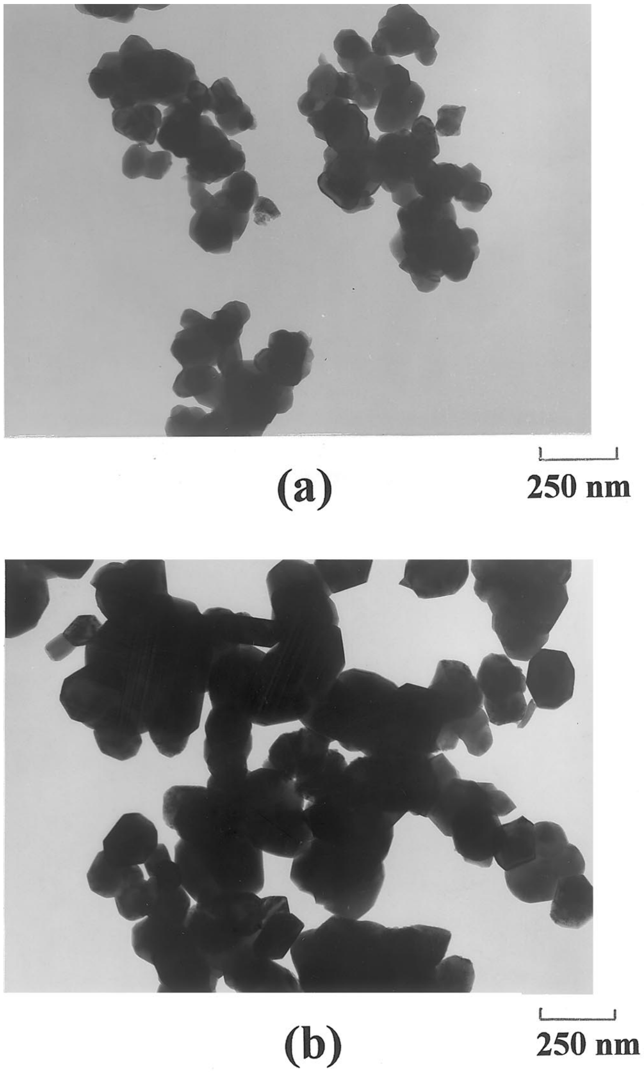

Fig. 2. Transmission electron micrographs of 800°C-calcined $LiMn_2O_4$ powders from solutions having the molar ratio of the metal ions to the monomer units of PVA equal to (a) 1:2 (sample A) and (b) 2:1 (sample B).

plateaus in the discharge curves. This is due to two-step reduction and oxidation process, which is a characteristic of lithium manganese oxide spinel [18,19]. The charge–discharge profile (Fig. 3(a)) shows that the electrochemical behavior of the powder exhibits an initial discharge capacity of 124 mA h g^{-1} at 25°C. An elevated temperature operation at 55°C reduces the initial discharge capacity to 111 mA h g^{-1}. The charge–discharge electrochemical behavior of 800°C-calcined powders of sample B is illustrated in Fig. 4. The initial discharge capacity is relatively lower with respect to sample A at both operation temperatures of 25°C and 55°C. The initial discharge capacity of sample B at 25°C is 109 mA h g^{-1}, and is reduced to 104 mA h g^{-1} at 55°C. The variation of initial charge–discharge capacity for different samples is considered to result from the difference in the particle size of $LiMn_2O_4$ powders. When the particle size is reduced, the overall surface area is increased. Thus, the cathode composed of small particles with large interface area can provide more lithium ions for diffusion, and therefore the specific capacity is increased.

Variation of the specific discharge capacity with the cycle number is elucidated in Fig. 5. As shown in Fig. 5(a), the capacity losses over 10 cycles for the 800°C-calcined $LiMn_2O_4$ powders obtained from samples A and B at 25°C are 10% and 4% of the initial discharge capacity, respectively. When the operation temperature is raised to 55°C, the capacity loss for sample B over 10 cycles is around 4%; however, the capacity loss for sample A is markedly increased to 20%. Apparently, sample A suffers serious capacity fading at elevated

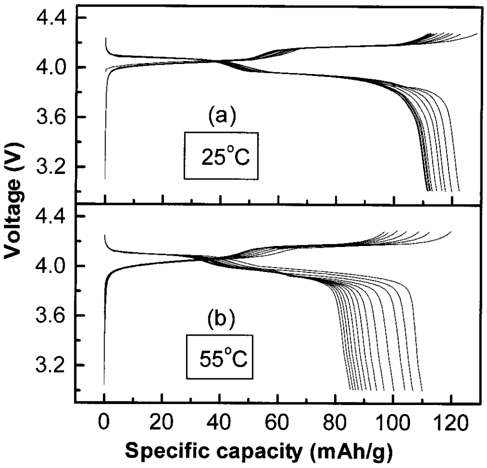

Fig. 3. Cycling charge/discharge curves over the potential range of 3.0 to 4.3 V at a current density of 0.2 mA cm^{-2} using $LiMn_2O_4$. 800°C-calcined powders of sample A, operated at (a) 25°C and (b) 55°C.

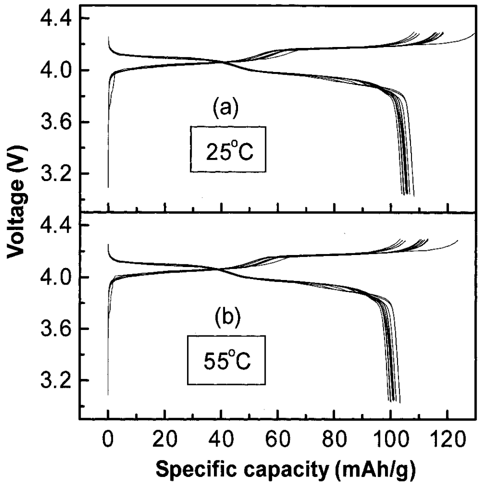

Fig. 4. Cycling charge/discharge curves over the potential range of 3.0 to 4.3 V at a current density of 0.2 mA cm^{-2} using $LiMn_2O_4$. 800°C-calcined powders of sample B, operated at (a) 25°C and (b) 55°C.

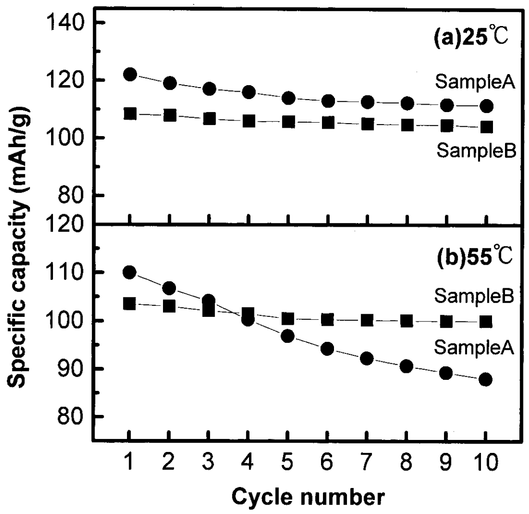

Fig. 5. Variation of the specific discharge capacity with the cycle number for 800°C-calcined powders of samples A and B at (a) 25°C and (b) 55°C.

temperatures. The faster capacity fading for sample A is possibly related to smaller particle size of $LiMn_2O_4$ powders. Small particles provide more surface area for lithium ions to diffuse in and out of the host structure; however, the large surface area also enhances the reactivity between $LiMn_2O_4$ particles and electrolyte, which reduces the structure stability of the spinel phase during charge–discharge cycling. Consequently, optimization of the particle size of $LiMn_2O_4$ powders by different synthesis processes is crucial for increasing the discharge capacity and tailoring the cyclability at elevated temperatures.

4. Conclusions

Spinel $LiMn_2O_4$ powders have been synthesized by a sol–gel method using an aqueous solution of metal nitrates containing PVA as a gelling agent. The $LiMn_2O_4$ powders obtained by this process have an uniform morphology with a narrow size distribution. The average particle size of $LiMn_2O_4$ powder decreases with an increase in the PVA amount used in the precursor solution. The obtained powders exhibit good electrochemical properties as cathode materials for the application to Li-ion batteries. $LiMn_2O_4$ particles with small particle size have large initial discharge capacity at room temperature, but fast fading rate of capacity at elevated temperature of operation. Controlling the particle size of $LiMn_2O_4$ during synthesis processes is important for raising the discharge capacity and improving the cyclability at elevated temperatures.

References

[1] G. Pistoia, A. Antonini, R. Rosati, D. Zane, Electrochem. Acta 41 (1996) 1683.
[2] K. Miura, A. Yamada, M. Tanaka, Electrochem. Acta 41 (1996) 249.
[3] J.M. Tarascon, D. Guyomard, Electrochem. Acta 38 (1993) 1221.
[4] J.N. Reimers, J.R. Dahn, J. Electrochem. Soc. 139 (1992) 2091.
[5] C.D.W. Jones, E. Rossen, J.R. Dahn, Solid St. Ionics 68 (1994) 65.
[6] J. Barker, R. Kockbang, M.Y. Saidi, Solid St. Ionics 89 (1996) 25.
[7] J.M. Tarascon, E. Wang, F.K. Shokoohi, W.R. McKinnon, S. Colson, J. Electrochem. Soc. 137 (1991) 2859.
[8] Z. Jiang, K.M. Abraham, J. Electrochem. Soc. 143 (1996) 1591.
[9] X. Qiu, X. Sun, W. Shen, N. Chen, Solid St. Ionics 93 (1997) 335.
[10] K.T. Hwang, W.S. Um, H.S. Lee, J.K. Song, K.W. Chung, J. Pow. Sources 74 (1998) 169.
[11] S.T. Myung, H.T. Chung, J. Pow. Sources 84 (1999) 32.
[12] Y.H. Ikuhara, Y Iwamoto, K. Kikuta, S. Hirano, J. Mater. Res. 14 (1999) 3102.
[13] W. Liu, K. Kowal, G.C. Farrington, J. Electrochem. Soc. 143 (1996) 3590.
[14] S.K. Saha, A. Pathak, P. Pramanik, J. Mater. Sci. Lett. 14 (1995) 35.
[15] M.A. Gulgun, M.H. Nguyen, W.M. Kriven, J. Am. Ceram. Soc. 82 (1999) 556.
[16] S.K. Saha, P. Pramanik, Brit. Ceram. Trans. 94 (1995) 123.
[17] S.K. Saha, P. Pramanik, Nanostru. Mater. 8 (1997) 29.
[18] M.M. Thackeray, W.I.F. David, P.G. Bruce, J.B. Goodenough, Mater. Res. Bull. 18 (1993) 461.
[19] Y.M. Choi, S.I. Pyun, Solid St. Ionics 99 (1997) 173.